

1 Revisiting Day-of-Week Ozone Patterns in an Era of Evolving U.S. 2 Air Quality

3 Heather Simon¹, Christian Hogrefe², Andrew Whitehill², Kristen M. Foley², Jennifer Liljegren³,
4 Norm Possiel¹, Benjamin Wells¹, Barron H. Henderson¹, Lukas C. Valin², Gail Tonnesen⁴, K.
5 Wyatt Appel², Shannon Koplitz¹

6
7 ¹US Environmental Protection Agency, Office of Air and Radiation, Research Triangle Park, NC

8 ²US Environmental Protection Agency, Office of Research and Development, Research Triangle Park, NC

9 ³US Environmental Protection Agency, Region 5, Chicago, IL

10 ⁴US Environmental Protection Agency, Region 8, Denver, CO

11 *Correspondence to:* Heather Simon (Simon.Heather@epa.gov)

12
13 **Abstract.** Past work has shown that traffic patterns in the US and resulting NO_x emissions vary by day of week, with
14 NO_x emissions typically higher on weekdays than weekends. This pattern of emissions leads to different levels of
15 ozone on weekends versus weekdays and can be leveraged to understand how local ozone formation changes in
16 response to NO_x emissions perturbations in different urban areas. Specifically, areas with lower NO_x but higher ozone
17 on the weekends (the weekend effect) can be characterized as NO_x-saturated and areas with both lower NO_x and
18 ozone on weekends (the weekday effect) can be characterized as NO_x-limited. In this analysis we assess maximum
19 daily 8-hr average (MDA8) ozone weekend-weekday differences across 51 US nonattainment areas using 18 years of
20 observed and modeled data from 2002-2019 using two metrics: mean MDA8 ozone and percentage of days with
21 MDA8 ozone > 70 ppb. In addition, we quantify the modeled and observed trends in these weekend-weekday
22 differences across this period of substantial NO_x emissions reductions in the US. The model assessment is carried out
23 using EPA's Air Quality Time Series Project (EQUATES) CMAQ dataset. We identify 3 types of MDA8 ozone
24 trends occurring across the US: transitioning chemical regime, disappearing weekday effect, and no trend. The
25 transitioning chemical regime trend occurs in a subset of large urban areas that were NO_x-saturated (i.e., VOC-
26 limited) at the beginning of the analysis period but transitioned to mixed chemical regimes or NO_x-limited conditions
27 by the end of the analysis period. Nine areas have strong transitioning chemical regime trends using both modeled and
28 observed data and with both metrics indicating strong agreement that they are shifting to more NO_x-limited conditions:
29 Milwaukee, Houston, Phoenix, Denver, Northern Wasatch Front, Southern Wasatch Front, Las Vegas, Los Angeles –
30 San Bernardino County, Los Angeles – South Coast, and San Diego. The disappearing weekday effect was identified
31 for multiple rural and agricultural areas of California which were NO_x-limited for the entire analysis period but appear
32 to become less influenced by local day of week emission patterns in more recent years. Finally, we discuss a variety
33 of reasons why there are no trends in certain areas including complex impacts of heterogeneous source mixes and
34 stochastic impacts of meteorology. Overall, this assessment finds that the EQUATES modeling simulations indicate
35 more NO_x-saturated conditions than the observations but do a good job of capturing year-to-year changes in weekend-
36 weekday MDA8 ozone patterns.

38 **1 Introduction**

39 Ground-level ozone (O₃), a key component of photochemical smog, has adverse impacts on human health and
40 ecosystems (U.S. Environmental Protection Agency, 2019). In the United States (US), the Clean Air Act Amendments
41 of 1970 instruct the Environmental Protection Agency (EPA) to set National Ambient Air Quality Standards
42 (NAAQS) for criteria pollutants. Since 1979, O₃ has served as the indicator species for the criteria pollutant of
43 photochemical oxidants (44 FR 8202) and since 1997, the form of the standard has been determined by the 3-year
44 average of the annual 4th-highest daily maximum 8-hour concentration (MDA8) (62 FR 38856). In 2015, the O₃
45 NAAQS were revised to the current level of 0.070 ppm or 70 ppb (80 FR 65291). As of 2018, 52 areas in the US had
46 been designated as nonattainment of the 2015 O₃ NAAQS (83 FR 25776; 83 FR 35136; 83 FR 52157).

47
48 O₃ is predominantly a secondary pollutant formed from photochemical reactions of nitrogen oxides (NO_x) and volatile
49 organic compounds (VOCs). Ground-level O₃ concentrations are a complex nonlinear function of the chemistry of
50 natural and anthropogenic precursor emissions, as well as meteorology, transport, and deposition (Seinfeld and Pandis,
51 2016). O₃ formation rates depend on the concentrations and speciation of NO_x and VOCs. To reduce ambient O₃
52 concentrations, control strategies have been enacted in the US over the last 50 years to reduce the emissions of both
53 NO_x and VOCs (Simon et al., 2015).

54
55 The effectiveness of different control strategies on O₃ production rates depends on the photochemical environment
56 under which ozone is formed. Ozone formation environments are typically categorized as either NO_x-limited or NO_x-
57 saturated, with a mixed or transitional regime between the two (Sillman, 1995, 1999; Sillman et al., 1990). In the NO_x-
58 limited regime, ambient ozone concentrations will respond more strongly to changes in NO_x emissions than VOC
59 emissions. In contrast, in a NO_x-saturated (or VOC-limited) regime, ozone will increase with NO_x emission controls
60 but will decrease with VOC emissions controls. Understanding the photochemical regimes of different ozone
61 nonattainment areas and how they have changed over time is important for understanding the impacts of previous
62 control strategies and guiding future control strategies to have the maximum health benefit with the least economic
63 burden.

64
65 Different methods have been proposed to determine ozone formation regimes and their changes over time. One
66 common method used to evaluate ozone formation chemistry is through day-of-week (DOW) differences in the
67 concentration of ozone and its precursors. The DOW effects leverage NO_x emissions differences between weekdays
68 and weekends (Marr and Harley, 2002a, b). In the US, onroad vehicles are a dominant source of NO_x emissions (Toro
69 et al., 2021). Diesel vehicle traffic tends to be higher on weekdays (Monday through Friday) than on weekends
70 (Saturday and Sunday). This results in higher NO_x emissions on weekdays than weekends (Marr and Harley, 2002a,
71 b). Daily varying emissions sources such as diesel vehicles are not a major source of VOC emissions. In addition,
72 VOC emissions in some areas are dominated by biogenic emissions that do not vary by day of week. Consequently,
73 VOC emissions are generally similar on weekends and weekdays in most areas. The result of DOW NO_x patterns is
74 that ozone concentrations tend to be higher on weekends than weekdays in NO_x-saturated areas and lower on
75 weekends than weekdays in NO_x-limited areas (Kopplitz et al., 2022). DOW differences in ozone were first reported

76 in the 1970s (Bruntz et al., 1974; Cleveland et al., 1974). In 2002 the DOW ozone differences in California were
77 explicitly tied to DOW patterns in diesel vehicle traffic (Marr and Harley, 2002a, b). Since that time, multiple studies
78 have used DOW ozone patterns to assess ozone chemical formation regimes in individual US cities including Los
79 Angeles, California (Chinkin et al., 2003; Fujita et al., 2003b; Fujita et al., 2003a; Gao, 2007; Gao and Niemeier,
80 2007; Warneke et al., 2013), Fresno, California (De Foy et al., 2020), Sacramento, California (Murphy et al., 2007),
81 Phoenix, Arizona (Atkinson-Palombo et al., 2006), Atlanta, Georgia (Blanchard and Tanenbaum, 2006), Baltimore,
82 Maryland (Roberts et al., 2022), and New York City, New York (Singh and Kavouras, 2022). A smaller number of
83 studies have assessed ozone DOW patterns across multiple US urban areas (Blanchard et al., 2008; Jaffe et al., 2022;
84 Koo et al., 2012; Koplitz et al., 2022; Pun et al., 2003). Additionally, ozone DOW patterns have been used as a method
85 for assessing chemical formation regimes outside of the US in Shanghai, China (Zhang et al., 2023), the Lesser Antilles
86 Archipelago (Plocoste et al., 2018), Rio de Janeiro, Brazil (Martins et al., 2015), Santiago, Chile (Rubio et al., 2011),
87 Andalusia, Spain (Adame et al., 2014), the Iberian Peninsula (Jiménez et al., 2005), Athens, Greece (Paschalidou and
88 Kassomenos, 2004) and in multiple other European cities (Pires, 2012). One complication with interpreting DOW O₃
89 patterns is that O₃ concentrations in urban areas are generally impacted by a mix of transport and local formation. O₃
90 transport can occur over a variety of timescales. In some locations there could be a regional O₃ DOW effect that might
91 be evident as a slightly lagged timescale depending on typical transport times from major upwind urban source areas.

92
93 Previous work has shown a substantial decrease in NO_x emissions in the US over the past 20 years as a result of
94 national, state, and local regulations (Krotkov et al., 2016; Lamsal et al., 2015; Russell et al., 2012; Toro et al., 2021).
95 Concurrent with the US NO_x decreases, multiple studies have found that ozone chemical formation regimes have also
96 changed in the US (Jin et al., 2020; Jin et al., 2017; Koplitz et al., 2022). In this paper, we focus on 51 areas in the US
97 which were designated in 2018 as nonattainment ([https://www.epa.gov/green-book/green-book-8-hour-ozone-2015-](https://www.epa.gov/green-book/green-book-8-hour-ozone-2015-area-information)
98 [area-information](https://www.epa.gov/green-book/green-book-8-hour-ozone-2015-area-information)) under the 2015 O₃ NAAQS (some of these areas have since been redesignated to attainment based
99 on clean monitoring data). We look at changes in DOW patterns in the US over 18 years from 2002 to 2019 using
100 both measured and modeled data to provide insights into how ozone formation chemistry has changed in the US as a
101 result of emissions reductions, and to assess how well modeling is able to capture the observed changes. This 18-year
102 dataset, which is part of EPA's Air QUALity Time Series Project (EQUATES), is unique in its application of consistent
103 emissions and modeling methodologies across the entire analysis period providing an opportunity to assess multi-year
104 trends.

105

106 **2 Methods**

107
108 For this assessment we use MDA8 ozone monitoring data obtained from EPA's Air Quality System (AQS)
109 (<https://www.epa.gov/aqs>) and MDA8 ozone modeling data from simulations of the Community Multiscale Air
110 Quality model version 5.3.2 (CMAQv5.3.2). The CMAQ model data are part of EQUATES which provides an 18-
111 year set of modeled meteorology, emissions, air quality and pollutant deposition spanning the years 2002 through
112 2019 using consistent modeling methods across years. The CMAQv5.3.2 model configuration, including input data,

113 boundary conditions, and science options are available from US EPA (EPA, 2021). The emissions inventories
114 developed for the EQUATES CMAQ modeling are described in (Foley et al., 2023).

115
116 We extract CMAQ modeling data only for days and grid-cells with monitoring data such that both datasets are paired
117 in time and location. Both datasets are subset to ozone monitors located within 51 of the 52 areas that were designated
118 in 2018 as nonattainment for the 2015 O₃ NAAQS (a list of areas is available in Tables S1 and S2) (83 FR 25776; 83
119 FR 35136; 83 FR 52157). Because this analysis focuses on May-September data, we do not include data from the
120 Uintah Basin nonattainment area for which violations of the NAAQS predominantly occur in winter months. Data are
121 analyzed for the 18-year period of the EQUATES modeling dataset.

122
123 We start by analyzing changes in MDA8 ozone between weekends and weekdays pooled across all monitoring
124 locations for each nonattainment area for 5-year rolling periods (i.e., 14 different periods covering the 18-year
125 timeseries). We pool data into 5-year periods for several reasons. First, it dampens impacts of interannual meteorology
126 that can contribute to large year-to-year changes in ozone for a given location. Previous work has shown that
127 differential meteorological patterns on weekends versus weekdays impacts ozone DOW patterns in a single year and
128 that pooling data across multiple years can reduce this effect (Pierce et al., 2010). Second, it provides a larger sample
129 size for calculating ozone differences between weekends and weekdays. The use of 5-year periods does, however,
130 limit this analysis' ability to parse out changes in weekend-weekday differences that have occurred due to emissions
131 changes in the most recent individual years analyzed. For example, any changes occurring only in 2018 and/or 2019
132 would be dampened in the 2015-2019 pooled data.

133
134 For the purpose of quantifying differences in weekend versus weekday O₃ concentrations, we use Sundays to represent
135 weekends (WE) and Tuesdays, Wednesdays and Thursdays to represent weekdays (WD). We do not include ozone
136 on Monday and Saturday to minimize any carryover impacts on concentrations from the previous day and we exclude
137 Friday as it may exhibit somewhat different emissions patterns than the other weekdays.

138
139 We use two metrics to quantify differences in MDA8 ozone between weekends and weekdays. First, we quantify mean
140 differences in MDA8 ozone across the entire distribution of days in each season (Winter = Dec, Jan, Feb; Spring =
141 Mar, Apr, May, Summer = Jun, Jul, Aug, Fall = Sep, Oct, Nov, ozone season = May-Sep) using Eq. (1), where O_{3,WE}
142 represents MDA8 O₃ on Sundays and O_{3,WD} represents MDA8 O₃ on Tuesdays, Wednesdays, and Thursdays.

143
144
$$\overline{\Delta O_{3,DOW}} = \overline{O_{3,WE}} - \overline{O_{3,WD}} \quad (1)$$

145
146 In this study we mainly focus on differences during the May-Sep ozone season. The Welch's t-test (Welch, 1947) is
147 used to denote whether the mean WE-WD difference is statistically different from zero ($p < 0.05$). Within each
148 nonattainment area, the t-test calculation was used to compare the means of every weekday and every weekend day
149 in a 5-year window, treating each day as an independent observation. All available ozone monitoring data and model

150 output from all monitoring locations within each nonattainment area are included in the calculation, providing a
151 measure of average behavior across each area. We also examine 24-hour average modeled formaldehyde and NO_x
152 concentrations at each of the ozone monitor locations to verify whether the model shows expected patterns of higher
153 NO_x on weekdays than on weekends and trends in these ozone precursors. Formaldehyde is used as an indicator of
154 first-generation VOC reaction products for this purpose. We note that monitoring data for VOCs and NO_x are much
155 sparser in terms of sampling frequency and spatial density than ozone measurements, so we rely on the model alone
156 to verify underlying day-of-week patterns in precursor compounds.

157
158 Second, similar to (Jaffe et al., 2022), we look at the percent of days with MDA8 ozone values above the NAAQS
159 level of 70 ppb. We calculate the percent of total weekends and weekdays in May-Sep for which MDA8 ozone
160 concentrations exceeded 70 ppb as shown in Eq. (2).

$$161 \Delta O_{3,DOW,\%>70} = O_{3,WE,\%>70} - O_{3,WD,\%>70} \quad (2)$$

162
163 For this calculation, a day is characterized as exceeding the NAAQS in an area if measured and/or modeled MDA8
164 ozone is above 70 ppb at the location of any ozone monitor within the area. In this way we are tracking days where
165 some portion of the area has observed or modeled MDA8 ozone above 70 ppb, but the analysis does not distinguish
166 whether the high ozone concentrations are localized over a small portion of the area or widespread across multiple
167 monitoring locations. This analysis also does not consider whether days with modeled MDA8 ozone above 70 ppb
168 occur simultaneously with observed MDA8 ozone above 70 ppb. We use the Fisher's exact test (Fisher, 1935; Mehta
169 and Patel, 1983) to determine whether the proportion of days above 70 ppb differs between weekends and weekdays.

170
171 Next, we use the Theil-Sen estimator (Sen, 1968; Theil, 1992) to determine the multi-year trends in $\overline{\Delta O_{3,DOW}}$ and
172 $\Delta O_{3,DOW,\%>70}$ for each area. This nonparametric approach was chosen due to the small sample size (n=14 5-year
173 windows) and the fact that the Theil-Sen estimator does not require any assumptions on the distribution of the
174 residuals. The Mann-Kendall test (Kendall, 1975; Mann, 1945) is used to determine the statistical significance of the
175 derived trends in WE-WD MDA8 O₃ differences. For each derived trend, we also document the 95% confidence
176 interval. Because we use a 5-year rolling window for each area, the individual data points in the trends analysis are
177 correlated. While this should not systematically bias the calculated slopes, it will lead to lower P-values and narrower
178 95% confidence intervals than would be calculated if the data points were uncorrelated. However, the P-value is still
179 informative to characterize which areas have the strongest trends. Therefore, while we do report P-values we do not
180 rely on a strict threshold for determining statistical significance.

181
182 Finally, investigation of relationships between WE-WD MDA8 O₃ and meteorological parameters used the
183 meteorological dataset developed by and described in (Wells et al., 2021). Meteorological parameters were similarly
184 compared across weekends and weekdays, matching times and locations of the ozone analysis and using the same
185 statistical methods for comparison.
186

187
188
189
190
191
192
193
194
195
196
197
198
199
200
201
202
203
204
205
206
207
208
209
210
211
212
213
214
215
216
217
218
219
220
221
222

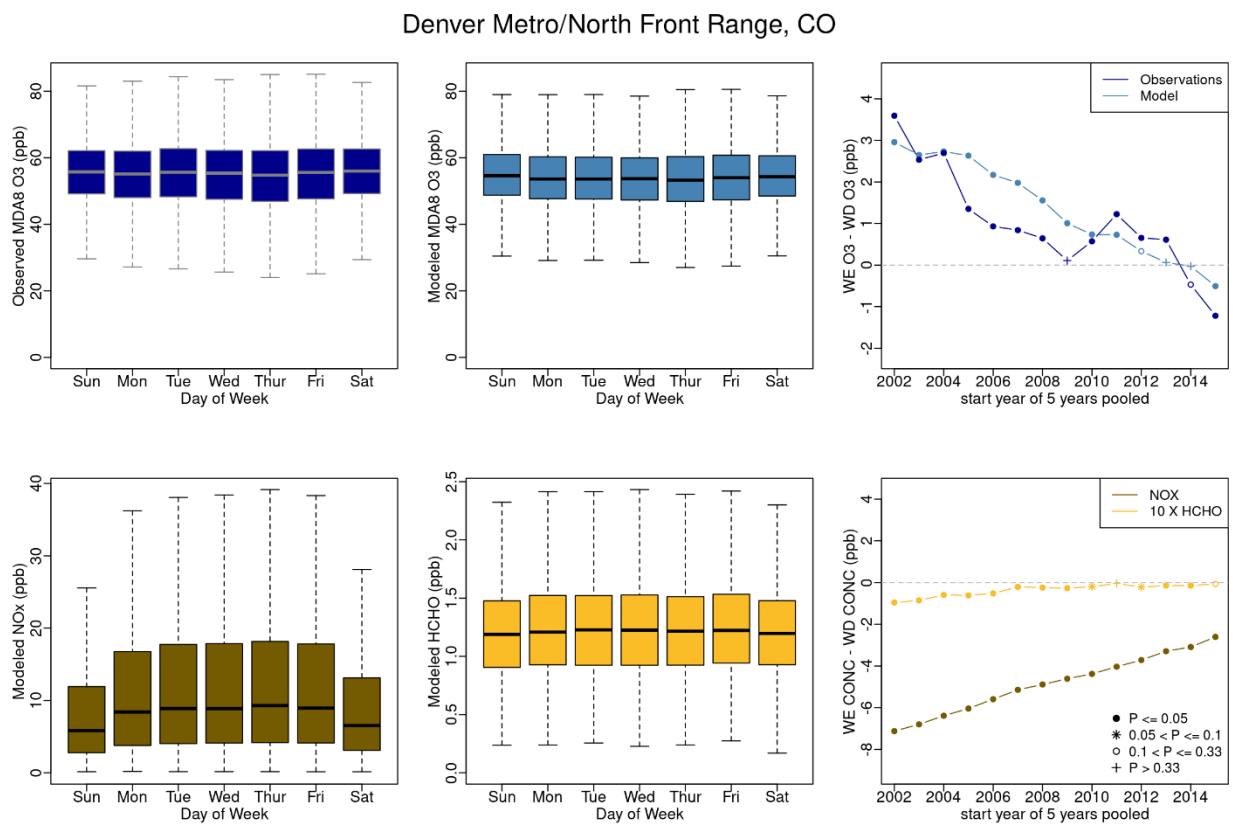
3 Results

3.1 Modeled NO_x and formaldehyde day-of-week patterns

We first look at modeled NO_x and formaldehyde day-of-week patterns to better understand how daily changes in precursor emissions impact modeled day-of-week ozone patterns. We chose to focus on modeled data here because of the ubiquitous spatial and temporal coverage provided in the model for these pollutants allowing us to evaluate these pollutants on the same days and at the same locations as the ozone monitors. We note that some observed NO_x data can also be used for this purpose, although NO_x data are not available for all nonattainment areas and are not available at the locations of all ozone monitors even within nonattainment areas with NO_x monitoring data. A comparison of monitored and observed trends in NO_x day-of-week differences provided in Figures S-1 through S-26 shows that the model does reasonably well at capturing the patterns in the limited observational dataset that is available. Due to the sparsity of formaldehyde measurements, both spatially and temporally (formaldehyde is commonly measured at a 1-in-6 day or 1-in-12 day frequency), a similar comparison cannot be made for modeled and measured formaldehyde. However, with more recent requirements for formaldehyde measurements at Photochemical Assessment Monitoring Stations (PAMS) locations starting in the 2017-2019 time-period, future assessments may have additional measured formaldehyde data that could be used for this purpose.

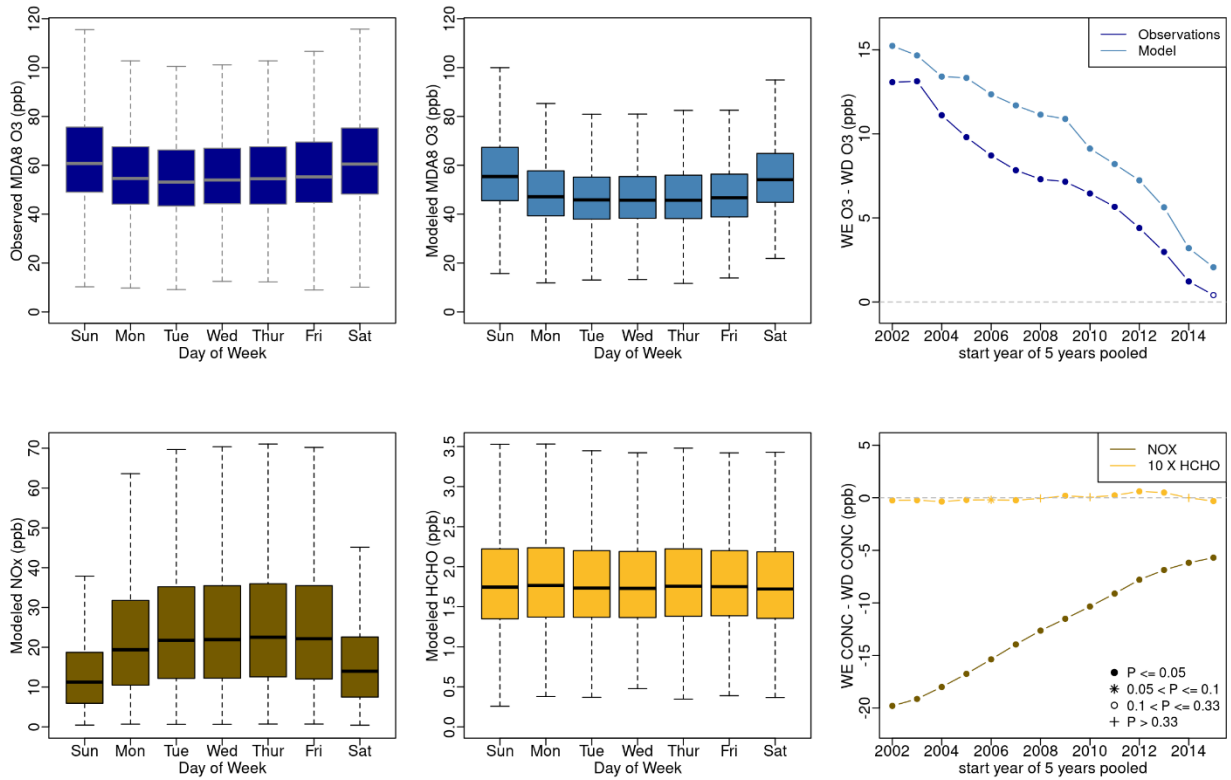
Utilizing the complete model data set, we see clear patterns of higher NO_x concentrations on weekdays than weekends for all but one of the 51 areas and relatively constant formaldehyde concentrations across May-Sep days for the entire 2002-2019 analysis period. This is consistent with the underlying assumption in the ozone day-of-week analyses discussed above. Here we describe examples of the modeled NO_x and formaldehyde day of week patterns using the data for Denver, CO and Los Angeles, CA to show typical patterns in large urban areas and Butte County, CA to show a typical pattern in a more rural area in Figures 1, 2, and 3, respectively. The modeled WE-WD differences in NO_x concentrations are more pronounced in large urban areas such as Los Angeles and Denver than in rural or agricultural areas such as Butte County. The only area that does not demonstrate higher modeled NO_x concentrations on weekdays than weekends is Door County, WI (Figure S-27). Higher NO_x emissions on weekdays are typically associated with commuting patterns and greater vehicular activity from commercial truck traffic. The nonattainment portion of Door County, which was fully redesignated to attainment in 2022 (87 FR 25410), is located at the tip of a peninsula on Lake Michigan and a rural recreation and tourist destination (i.e., likely to see more weekend activity). Consequently, the area does not follow typical weekday-weekend emission patterns and therefore modeled NO_x concentration patterns are unlike those of other areas. While the model does not predict substantial day-of-week formaldehyde differences in most areas, there are small modeled formaldehyde enhancements on weekdays compared to weekends in some areas such as Chicago (Figure S-28).

223 Theil-Sen trends show that differences in modeled WE versus WD NO_x have diminished over time in most areas (e.g.
 224 Figures 1, 2 and 3). The modeled WE versus WD differences in formaldehyde are also diminishing over time but to a
 225 much lesser extent. As total emissions have decreased, absolute modeled and observed concentrations of NO_x have
 226 also decreased along with the WE-WD differences in NO_x . Figures S-33 and S-34 show that the modeled WE versus
 227 WD NO_x trends remain whether tracking absolute or normalized NO_x differences in Denver and Los Angeles, which
 228 is consistent with modeled WE-WD NO_x trends seen in all but ten of the nonattainment areas. In nine of these areas
 229 (Houston, TX; Las Vegas, NV; Muskegon, MI; New York, NY; Phoenix, AZ; San Diego, CA; St. Louis, MO-IL;
 230 Tuolumne County, CA; and Yuma, AZ) absolute modeled WE-WD NO_x differences have diminished substantially
 231 but there is little change in relative WE-WD differences. In Mariposa County, CA neither absolute nor relative WE-
 232 WD NO_x differences have changed substantially between 2002-2019. These findings that NO_x concentrations and
 233 NO_x day-of-week patterns have decreased over time is consistent with national trends reported by (Jaffe et al., 2022).
 234
 235

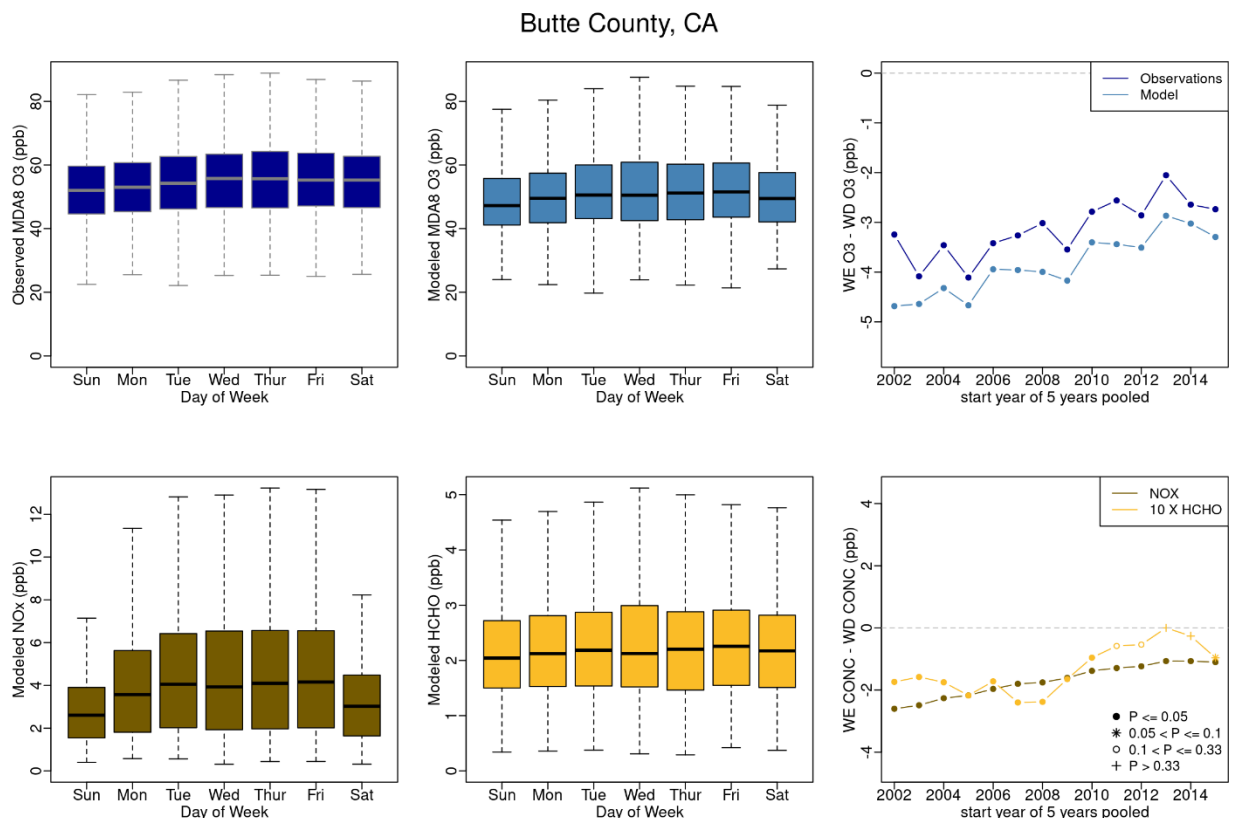


236
 237 **Figure 1. Denver area 2002-2019 May-Sep: observed (top left) and modeled (top center) MDA8 ozone distribution by day**
 238 **of week; modeled NO_x (bottom left) and modeled formaldehyde (bottom center) distribution by day of week; observed and**
 239 **modeled trends in $\Delta O_{3,DOW}$ (top right); modeled trends in WE-WD NO_x and formaldehyde differences (bottom right). The**
 240 **distributions by day of the week are for the entire 18 years with each box representing the 25th to 75th percentile for that**
 241 **day of the week across all 18 years, the whiskers representing the 1.5 times the interquartile range, and the bold line inside**
 242 **the box representing the median. WE-WD differences (top and bottom right) are based on 5-year rolling periods. P-values**
 243 **denoted by symbols in the right-hand panels refer to the t-test results comparing mean weekend and weekday values for**
 244 **each 5-year period.**
 245

Los Angeles-South Coast Air Basin, CA



246
 247 **Figure 2. Los Angeles area 2002-2019 May-Sep: observed (top left) and modeled (top center) MDA8 ozone distribution by**
 248 **day of week; modeled NO_x (bottom left) and modeled formaldehyde (bottom center) distribution by day of week; observed**
 249 **and modeled trends in $\Delta O_{3,DOW}$ (top right); modeled trends in WE-WD NO_x and formaldehyde differences (bottom right).**
 250 **The distributions by day of the week are for the entire 18 years with each box representing the 25th to 75th percentile for**
 251 **that day of the week across all 18 years, the whiskers representing the 1.5 times the interquartile range, and the bold line**
 252 **inside the box representing the median. WE-WD differences (top and bottom right) are based on 5-year rolling periods. P-**
 253 **values denoted by symbols in the right-hand panels refer to the t-test results comparing mean weekend and weekday values**
 254 **for each 5-year period.**
 255



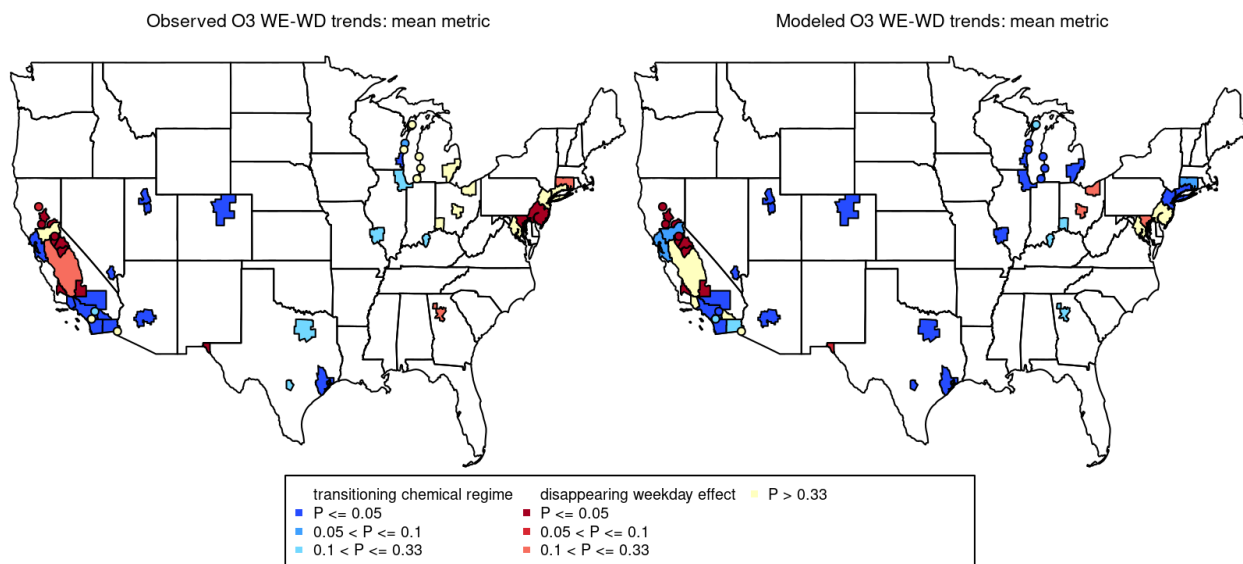
256
 257 **Figure 3. Butte County, CA area 2002-2019 May-Sep: observed (top left) and modeled (top center) MDA8 ozone distribution**
 258 **by day of week; modeled NO_x (bottom left) and modeled formaldehyde (bottom center) distribution by day of week;**
 259 **observed and modeled trends in $\Delta O_{3,DOW}$ (top right); modeled trends in WE-WD NO_x and formaldehyde differences**
 260 **(bottom right). The distributions by day of the week are for the entire 18 years with each box representing the 25th to 75th**
 261 **percentile for that day of the week across all 18 years, the whiskers representing the 1.5 times the interquartile range, and**
 262 **the bold line inside the box representing the median. WE-WD differences (top and bottom right) are based on 5-year rolling**
 263 **periods. P-values denoted by symbols in the right-hand panels refer to the t-test results comparing mean weekend and**
 264 **weekday values for each 5-year period.**
 265

266 3.2 Trend types of ozone day-of-week patterns

267
 268 Within any 5-year window, NO_x-saturated areas display a “weekend effect” meaning that MDA8 ozone
 269 concentrations were higher on weekends than on weekdays and NO_x-limited areas display a “weekday effect”
 270 meaning that ozone concentrations were higher on weekdays than on weekends. We categorize the trends in MDA8
 271 ozone DOW patterns into 3 discrete categories: 1) transitioning chemical regime (i.e. areas that went from NO_x-
 272 saturated to NO_x-limited), 2) disappearing weekday effect (i.e. areas that went from NO_x-limited to approaching zero
 273 in terms of DOW differences), and 3) areas with no trend over the 18-year time period. Transitioning chemical regime
 274 areas are characterized by a negative Theil-Sen slope (e.g. Denver and Los Angeles in Figures 1 and 2 respectively).
 275 Disappearing weekday effect areas are characterized by a positive Theil-Sen slope (e.g. Butte County in Figure 3).
 276 Areas with no trend are characterized by P-values > 0.33 as determined by the Mann-Kendall test. Trend types for all
 277 51 areas based on observed and modeled datasets are shown in Figure 4 and 5. Areas are color-coded by P-value
 278 ranges for both the transitional chemical regime trend type and the disappearing weekday effect trend type. Given the

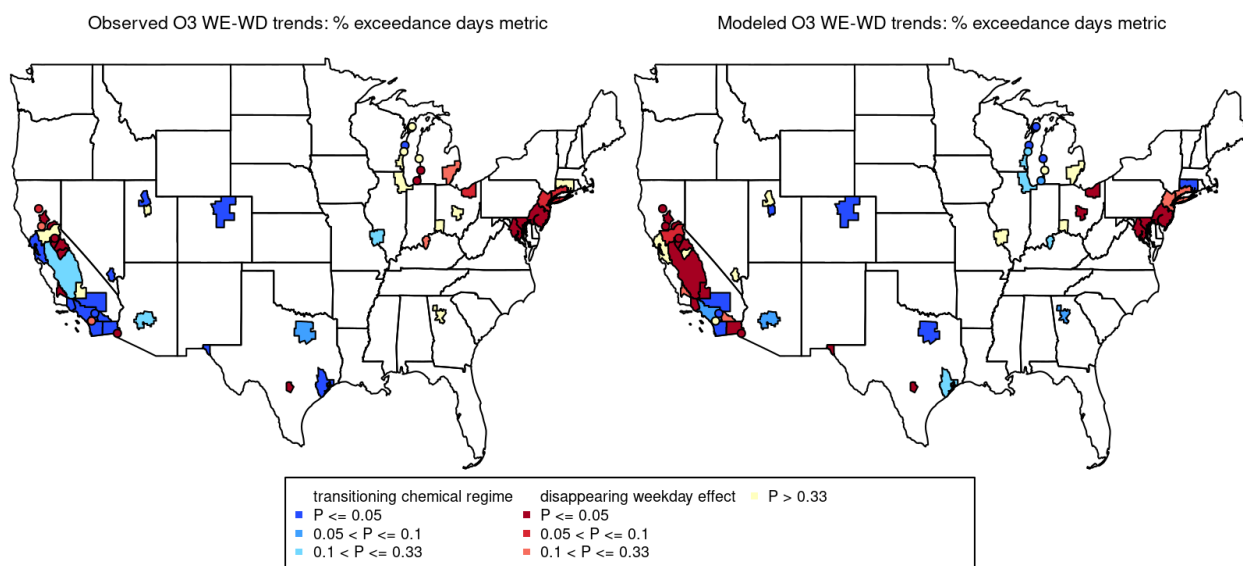
279 autocorrelation of the timeseries data we do not apply any strict P-value thresholds for identifying these trend types
 280 but we do note that areas with lower P-values show stronger trends than those with higher P-values.

281
 282



283
 284 **Figure 4. Map of ozone nonattainment areas color coded by trends in mean MDA8 ozone day of week differences ($\Delta\bar{O}_{3,DOW}$)**
 285 **using observed data (left) and modeled data (right) over an 18-year period from 2002-2019. Ozone nonattainment areas less**
 286 **than 3000 km² in area are shown as dots on the map for visibility.**

287
 288



289
 290 **Figure 5. Map of ozone nonattainment areas color coded by trends in ozone day of week differences based on the percentage**
 291 **of days with MDA8 ozone >70 ppb ($\Delta O_{3,DOW,\%>70}$) using observed data (left) and modeled data (right) over an 18-year**
 292 **period from 2002-2019. Ozone nonattainment areas less than 3000 km² in area are shown as dots on the map for visibility.**
 293

294 3.2.1 “Transitioning chemical regime” case studies 295

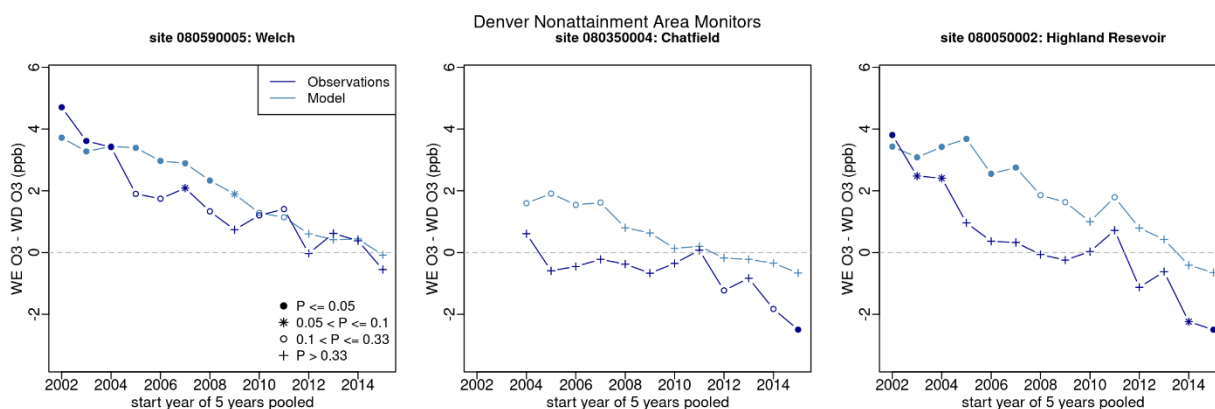
296 The transitioning chemical regime trend is typical of areas that initially had strongly positive ozone WE-WD
297 differences (i.e., mean MDA8 ozone is higher on weekends than on weekdays), suggesting NO_x-saturated conditions,
298 at the beginning of the analysis period. These areas typically transition into near-zero or negative WE-WD MDA8 O₃
299 differences by the most recent 5-year window, suggesting a shift to NO_x-limited conditions by the end of the analysis
300 period. Of the 51 nonattainment areas analyzed, 21 exhibit this type of trend for the $\overline{\Delta O_{3,DOW}}$ metric based on observed
301 data (14 with P-Values < 0.05, 1 with a P-Value between 0.05 and 0.1 and 6 with P-Values between 0.1 and 0.33) and
302 31 based on modeled data (22 with P-Values < 0.05, 3 with P-Values between 0.05 and 0.1 and 6 with P-Values
303 between 0.1 and 0.33). Of the 51 nonattainment areas analyzed, 17 exhibit this type of trend for the $\Delta O_{3,DOW,\%>70}$
304 metric based on observed data (14 with P-Values < 0.05 and 3 with P-Values between 0.1 and 0.33) and 19 based on
305 modeled data (10 with P-Values < 0.05, 4 with P-Values between 0.05 and 0.1 and 5 with P-Values between 0.1 and
306 0.33). This type of trend is consistent with previously reported national DOW trends reported across major
307 metropolitan areas using only the $\Delta O_{3,DOW,\%>70}$ metric (Jaffe et al., 2022).

308
309 Two areas that exhibit this trend for $\overline{\Delta O_{3,DOW}}$ are Denver and Los Angeles shown in Figures 1 and 2 respectively.
310 Modeled and observed $\overline{\Delta O_{3,DOW}}$ was in the range of +3 to +4 ppb at the beginning of the analysis period for Denver.
311 Both the observed and model data have decreasing Theil-Sen slopes for $\overline{\Delta O_{3,DOW}}$, -0.23 (observed) and -0.29
312 (modeled) ppb/yr with P-Values less than 0.001.. In the most recent 2015-2019 5-year window, both modeled and
313 observed $\overline{\Delta O_{3,DOW}}$ are negative, suggesting a shift to NO_x-limited conditions. While the results shown in Figure 1
314 represent aggregated measured MDA8 ozone data across all Denver nonattainment area monitors, Figure 6 shows
315 behavior at three specific monitors in Denver with monitoring records covering the majority of the analysis period.
316 All three sites were located to the south and southwest of the Denver urban area. The Welch monitor is located closer
317 to the Denver urban area in proximity to two major highways. While the negative observed and modeled Theil-Sen
318 slopes for $\overline{\Delta O_{3,DOW}}$ hold at all 3 sites, there are differences in the magnitude of the slopes and the sign of
319 $\overline{\Delta O_{3,DOW}}$ across sites. For instance, the Welch and Highland Reservoir sites both have positive $\overline{\Delta O_{3,DOW}}$ at the
320 beginning of the analysis period suggesting both sites were NO_x-saturated in the early 2000s. While the Chatfield site
321 had positive $\overline{\Delta O_{3,DOW}}$ at the beginning of the analysis period, larger P-Values indicate the differences may not be
322 statistically different from zero, suggesting that this location may have already been transitioning to NO_x-limited
323 conditions in the early-to-mid 2000s. The model predicts that all three sites have $\overline{\Delta O_{3,DOW}}$ that are negative but close
324 to zero at the end of the analysis period while observations show the substantial negative $\overline{\Delta O_{3,DOW}}$ values at Chatfield
325 and Highland Reservoir. This suggests that the model may understate the NO_x-limited conditions in recent years at
326 these locations. Los Angeles provides another example of an area where both the model and the observations had
327 strongly positive $\overline{\Delta O_{3,DOW}}$ at the beginning of the analysis period (+13 to + 15 ppb) and transitioning chemical regime
328 trends (Figure 2) with observed and modeled Theil-Sen slopes of 0.93 and 0.83 ppb/yr. Similar to Denver, site to site
329 differences in the magnitude of $\overline{\Delta O_{3,DOW}}$ are evident in Los Angeles (Figure S-33) but the transitioning chemical

330 regime trend is fairly consistent across sites. Similar types of trends in Chicago and Houston are shown in supplemental
 331 figures S-28 and S-29.

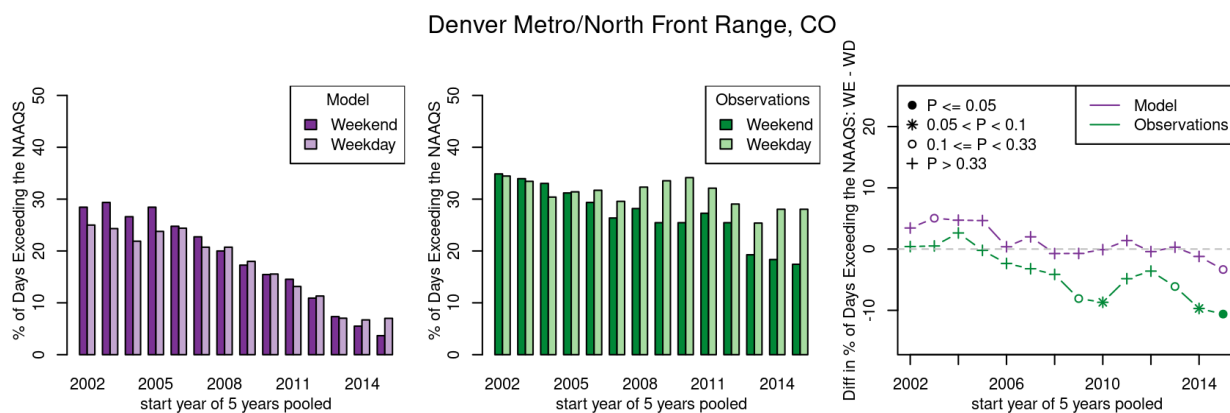
332
 333 In general, similar transitioning chemical regime trends in $\Delta O_{3,DOW,\%>70}$ are evident in Denver and Los Angeles
 334 (Figures 7 and 8). In both cases, the model underpredicts both the percentage of days with MDA8 $O_3 > 70$ ppb and
 335 the Theil-Sen slope. Additional examples of results for $\Delta O_{3,DOW,\%>70}$ are provided for Chicago, Houston and New
 336 York City in Figure S-35, S-36 and S-37 respectively.

337
 338
 339



340
 341 **Figure 6. Observed and modeled May-Sep trends in mean MDA8 ozone day of week differences ($\Delta \overline{O_{3,DOW}}$) at three Denver**
 342 **area monitoring locations for 2002-2019 plotted as 5-year rolling periods. P-values denoted by symbols refer to the t-test**
 343 **results comparing mean weekend and weekday values for each 5-year period.**
 344

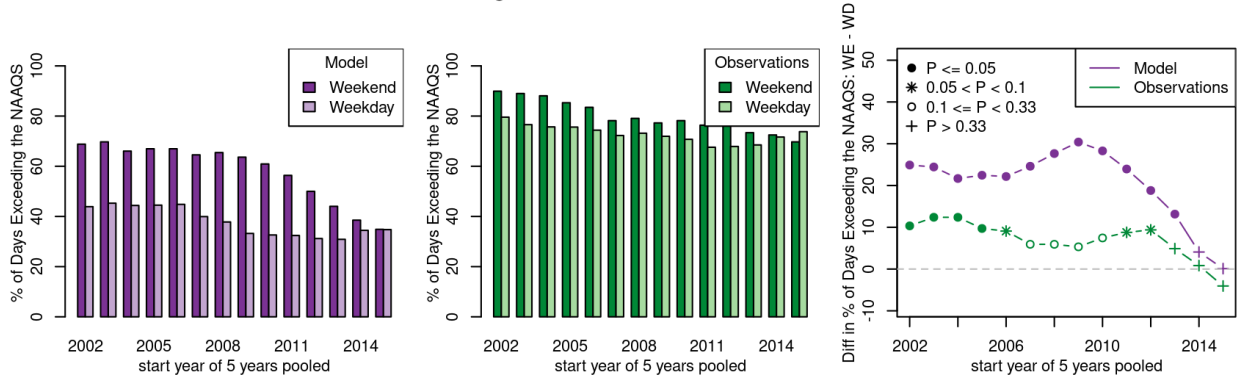
345



346
 347 **Figure 7. Modeled (left) and observed (center) percent of days with MDA8 ozone exceeding 70 ppb at any monitor within**
 348 **the Denver nonattainment area during May-Sep on weekends and weekdays for 5-year rolling periods between 2002-2019;**
 349 **Observed and modeled trends in May-Sep $\Delta O_{3,DOW,\%>70}$ at Denver area monitors for 5-year rolling periods between 2002-**
 350 **2019 (right). P-values denoted by symbols in the right-hand panel refer to the t-test results comparing mean weekend and**
 351 **weekday values for each 5-year period.**
 352

353
 354

Los Angeles-South Coast Air Basin, CA

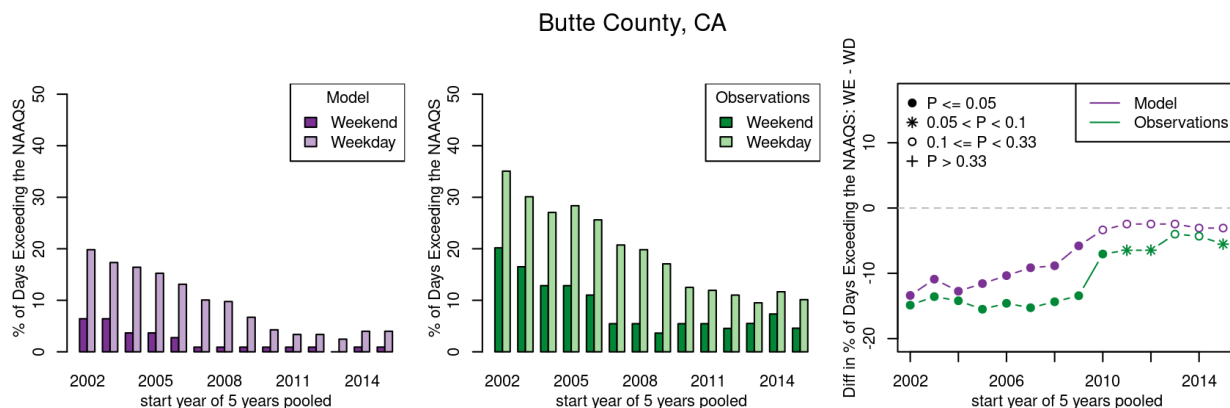


355
 356 **Figure 8. Modeled (left) and observed (center) percent of days with MDA8 ozone exceeding 70 ppb at any monitor within**
 357 **the Los Angeles nonattainment area during May-Sep on weekends and weekdays for 5-year rolling periods between 2002-**
 358 **2019; Observed and modeled trends in May-Sep $\Delta O_{3,DOW,\%>70}$ at Los Angeles area monitors for 5-year rolling periods**
 359 **between 2002-2019 (right). P-values denoted by symbols in the right-hand panel refer to the t-test results comparing mean**
 360 **weekend and weekday values for each 5-year period.**
 361

362 3.2.2 “Disappearing weekday effect” case study

363
 364 The disappearing weekday effect trend type in the $\overline{\Delta O_{3,DOW}}$ metric is evident in 16 out of the 51 nonattainment areas
 365 using observed data (12 with P-Values < 0.05, 1 with a P-Value between 0.05 and 0.1 and 3 with P-Values between
 366 0.1 and 0.33) and 13 out of the 51 nonattainment areas using modeled data (9 with P-Values < 0.05, 1 with a P-Value
 367 between 0.05 and 0.1 and 3 with P-Values between 0.1 and 0.33) (Figure 4). Of the 51 nonattainment areas analyzed,
 368 21 exhibit this type of trend for the $\Delta O_{3,DOW,\%>70}$ metric based on observed data (12 with P-Values < 0.05, 4 with P-
 369 Values between 0.05 and 0.1, and 5 with P-Values between 0.1 and 0.33) and 23 based on modeled data (17 with P-
 370 Values < 0.05, 1 with a P-Value between 0.05 and 0.1 and 5 with P-Values between 0.1 and 0.33) (Figure 5). This
 371 trend type is characterized by negative $\overline{\Delta O_{3,DOW}}$ values (i.e., weekday MDA8 ozone higher than weekend MDA8
 372 ozone) throughout the analysis period indicating NO_x-limited conditions trending upwards toward zero which appears
 373 primarily in rural/agricultural areas in California. The Butte County nonattainment area in California is one example
 374 of an area exhibiting this type of day-of-week trend pattern as is evident using both $\overline{\Delta O_{3,DOW}}$ and $\Delta O_{3,DOW,\%>70}$
 375 (Figures 3 and 9 respectively). The disappearing weekday effect could indicate that sources without day-of-week
 376 activity patterns are becoming more dominant contributors to local NO_x emissions. In that case, the day-of-week
 377 patterns for ambient NO_x concentrations are becoming less pronounced which would result in reductions in day-of-
 378 week MDA8 ozone patterns. An alternate explanation is that local NO_x emissions in general have decreased
 379 substantially enough that local ozone formation has become less important in such areas and a larger fraction of total
 380 ozone is being transported from upwind sources. In that case, the origin of the transported ozone could be a mixture
 381 of multiple source areas that are at varying distances upwind which could lead to a loss in the day-of-week ozone
 382 signal. More analysis would be needed to investigate this hypothesis with respect to nonattainment areas of interest.
 383 To our knowledge this trend type has not previously been reported in the literature although we note some previous
 384 national assessments (i.e., Jaffe et al., 2022) did not include many of the smaller rural and agricultural areas in
 385 California where this trend is most prevalent.

386
387



388
389 **Figure 9. Modeled (left) and observed (center) percent of days with MDA8 ozone exceeding 70 ppb at any monitor within**
390 **the Butte County, CA nonattainment area during May-Sep on weekends and weekdays for 5-year rolling periods between**
391 **2002-2019; Observed and modeled trends in May-Sep $\Delta O_{3,DOW,\%>70}$ at Butte County, CA area monitors for 5-year rolling**
392 **periods between 2002-2019 (right). P-values denoted by symbols in the right-hand panel refer to the t-test results comparing**
393 **mean weekend and weekday values for each 5-year period.**

394
395 **3.2.3 “No trend” case studies**

396
397 Out of the 51 nonattainment areas analyzed, 14 and 6 show no trend in the $\overline{\Delta O_{3,DOW}}$ metric using observed data and
398 modeled data respectively. Similarly, 12 and 9 show no trend in $\Delta O_{3,DOW,\%>70}$ using observed and modeled data
399 respectively. The reason for the lack of trends may vary by area. Plots for several areas are provided in the
400 supplemental information. Figures S-30, S-34 and S-37 provide the analysis for New York City which shows no trend
401 for the $\overline{\Delta O_{3,DOW}}$ using observations but a transitioning chemical regime trend for this metric using modeled data. Both
402 the model and the observations show a slight increasing trend in $\Delta O_{3,DOW,\%>70}$. One possible explanation for the lack
403 of trends in New York is the complex nature of the emissions sources and the meteorology impacting ozone formation
404 in this area. Figure S-34 shows $\overline{\Delta O_{3,DOW}}$ trends at three monitors in the New York City nonattainment area occurring
405 in very different locations. The Bronx IS 52 monitor, which is located in an urbanized part of the nonattainment area,
406 shows transitioning chemical regime in both modeled and observed $\overline{\Delta O_{3,DOW}}$. In contrast the Long Island – Riverhead
407 monitor and the Bridgeport CT monitor are both located in portions of the nonattainment area that are typically
408 downwind of the urban core on high ozone days and are impacted by complex meteorology associated with the land-
409 water interface near the Long Island sound. The modeled and observed data do not show substantial $\overline{\Delta O_{3,DOW}}$ trends
410 at the Long Island site and only the model shows transitioning chemical regime trends at the CT site. Due to the
411 complex nature of this large urban area, some sites may not show trends at all and trends at other sites may be masked
412 when aggregating data across a large number of sites.

413
414 Several nonattainment areas appear to have negative slopes in $\overline{\Delta O_{3,DOW}}$ at the beginning of the analysis period and
415 positive slopes at the end of the analysis period resulting in no overall trend over the entire period. Cincinnati, OH-
416 KY exemplifies this pattern and on closer inspection the patterns appear to mirror annual changes in WE-WD patterns

417 in multiple meteorological parameters (Figure S-38). For Cincinnati the correlation coefficients between WE-WD
418 MDA8 O₃ differences and WE-WD meteorological parameter differences were 0.77, -0.83, 0.79, 0.89, -0.94, and -
419 0.73 for daily maximum temperature, daily average relative humidity, daily maximum planetary boundary layer
420 height, solar radiation, percent cloud cover and 24-hour transport direction respectively. Other areas exhibiting this
421 behavior are all located in relatively close proximity to Cincinnati, including Louisville, KY-IN and St. Louis, MO-
422 IL and to a lesser extent Columbus, OH and Atlanta, GA. These findings suggest that for these areas even five-year
423 processing blocks may not be sufficient to remove the effects of spurious weekly meteorological variations on ozone.
424 Figure S-39 shows that the correlation between WE-WD differences in seven meteorological variables and observed
425 $\overline{\Delta O_{3,DOW}}$ do not appear to be a driving factor in significant $\overline{\Delta O_{3,DOW}}$ trends in other areas but it is possible that some
426 additional areas which do not have trends in $\overline{\Delta O_{3,DOW}}$ may also be impacted by meteorological variations.

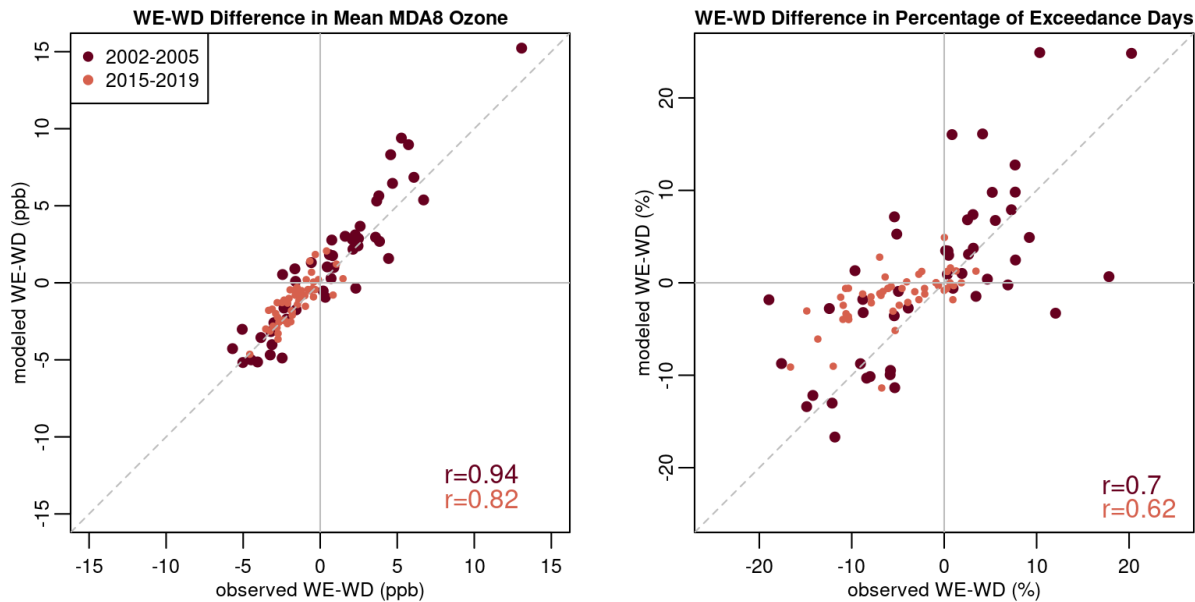
427

428 3.3 Comparison of modeled and observed trends in ozone day-of-week patterns

429

430 The modeled and observed trends in WE-WD differences for each of the 51 nonattainment areas are provided in
431 supplemental tables S1 ($\overline{\Delta O_{3,DOW}}$) and S2 ($\Delta O_{3,DOW,\%>70}$). Figure 10 provides a comparison of modeled to observed
432 WE-WD differences across the 51 nonattainment areas at the beginning of the analysis period (2002-2006) and at the
433 end of the analysis period (2015-2019). Each point represents the WE-WD MDA8 ozone difference for a single
434 nonattainment area, with the left-hand panel showing $\overline{\Delta O_{3,DOW}}$ and the right-hand panel showing $\Delta O_{3,DOW,\%>70}$. Data
435 points falling in the upper right quadrant of each panel represent areas for which both the observations and the modeled
436 DOW patterns suggest NO_x-saturated conditions. Data points in the lower left quadrant of each panel represent areas
437 for which both the observations and the model DOW patterns suggest NO_x-limited conditions. In the earlier 2002-
438 2006 time-period, there are a large number of areas falling in both the upper right and lower left quadrants for both
439 metrics. In the 2015-2019 time-period, almost all areas are located in the lower left quadrant for both metrics
440 suggesting that most US nonattainment areas have transitioned into NO_x-limited conditions. The correlation of
441 modeled and observed WE-WD differences is quite high ($r = 0.94$ and 0.82 for $\overline{\Delta O_{3,DOW}}$ in the earliest and most recent
442 time periods, respectively, and $r = 0.7$ and 0.62 for $\Delta O_{3,DOW,\%>70}$ in the earliest and most recent time periods,
443 respectively). For both metrics, the majority of points fall above the 1:1 line indicating that, in general, the model
444 overestimated the degree of NO_x-saturated conditions and underestimated the degree of NO_x-limited conditions.

445

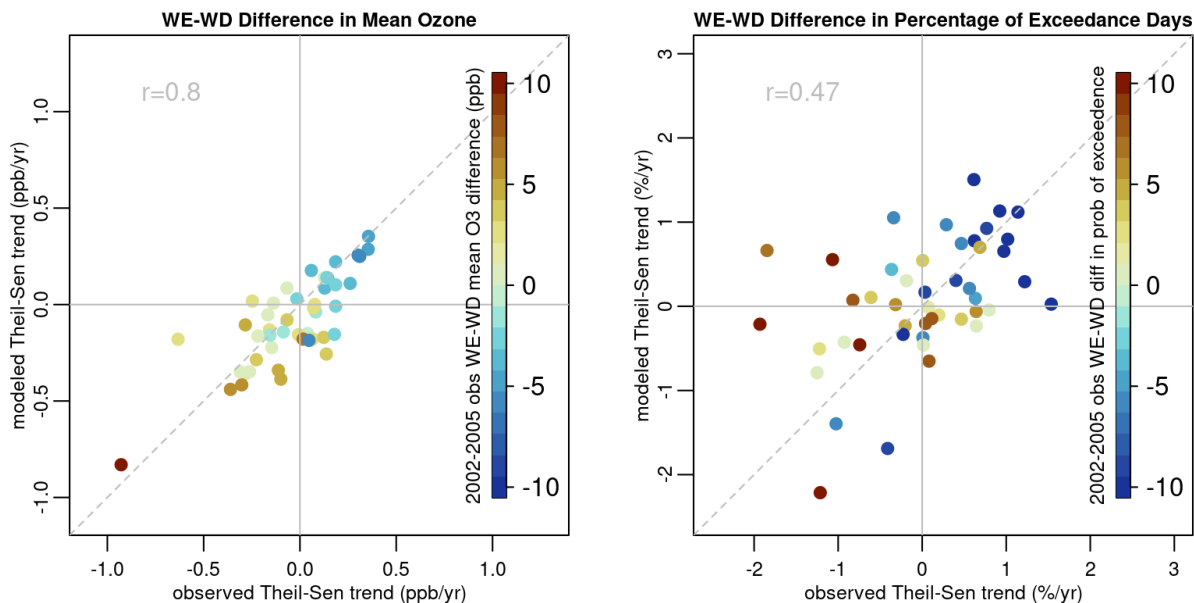


446
447 **Figure 10. Comparison of modeled and observed WE-WD MDA8 O₃ differences for $\overline{\Delta O_{3,DOW}}$ (left panel) and $\Delta O_{3,DOW,\%>70}$**
448 **(right panel). Differences shown for the 2002-2006 time period and for the 2015-2019 time period. Each dot represents a**
449 **different nonattainment area.**

450
451 Maps in Figures 4 and 5 show the locations of areas predicted to have transitioning chemical regime trends,
452 disappearing weekday effect trends and no trends for $\overline{\Delta O_{3,DOW}}$ and $\Delta O_{3,DOW,\%>70}$ respectively. The maps show
453 general consistency among which areas are predicted to have each trend type between observations and the model.
454 Nine areas are predicted to have transitioning chemical regime trends with P-Values < 0.05 in both datasets and with
455 both metrics indicating strong agreement that they are shifting to more NO_x-limited conditions: Milwaukee, WI;
456 Houston, TX; Phoenix, AZ; Denver, CO; Northern Wasatch Front, UT; Southern Wasatch Front, UT; Las Vegas, NV;
457 Los Angeles – San Bernardino County, CA; Los Angeles – South Coast, CA; and San Diego, CA.

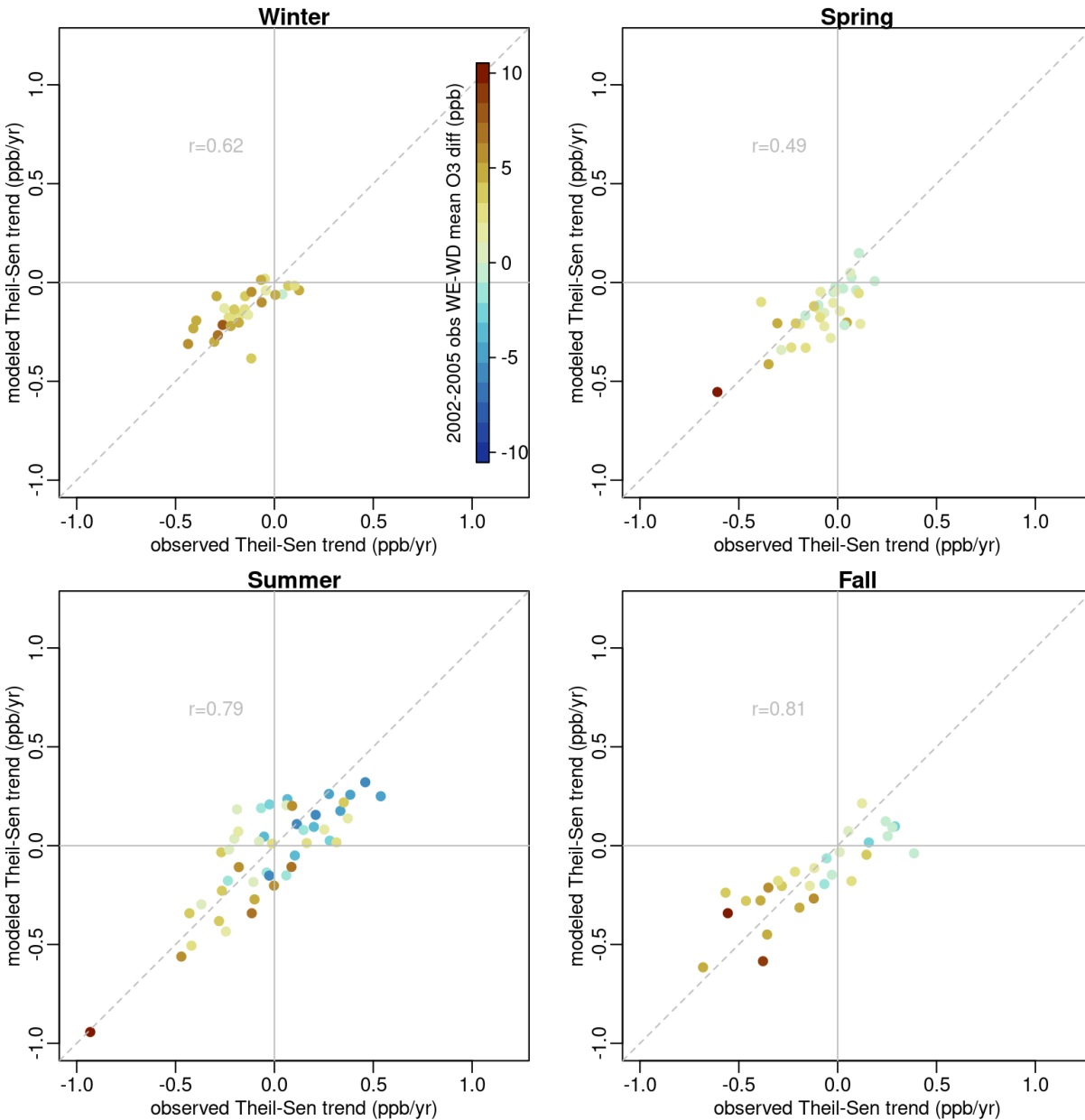
458
459 Figure 11 compares modeled and observed Theil-Sen slopes in WE-WD MDA8 O₃ differences across all areas. Each
460 point represents a single nonattainment area color-coded by 2002-2005 $\overline{\Delta O_{3,DOW}}$ or $\Delta O_{3,DOW,\%>70}$. The correlation of
461 modeled versus observed Theil-Sen slopes using $\overline{\Delta O_{3,DOW}}$ is stronger ($r = 0.8$) than the correlation using $\Delta O_{3,DOW,\%>70}$
462 ($r = 0.47$). While the model does not always correctly predict the Theil-Sen slope, the data falls close to the 1:1 line
463 for the $\overline{\Delta O_{3,DOW}}$ suggesting that the model does not systematically over or under predict the trends in WE-WD
464 differences from 2002-2019. The trend types described above for $\overline{\Delta O_{3,DOW}}$ metric are visible in the left-panel of Figure
465 11. Most NO_x-saturated areas (yellow and brown symbols) and some NO_x-limited areas (blue symbols) have negative
466 Theil-Sen slopes (i.e. transitioning chemical regime) towards NO_x-limited conditions similar to those described above
467 for Denver and Los Angeles (shown as the dark brown symbol at the bottom-left of the plot). Areas with positive
468 Theil-Sen slopes tend to be the most NO_x-limited areas (darker blue symbols) and represent the disappearing weekday
469 trends demonstrated by Butte County. The model is not as accurate at predicting $\Delta O_{3,DOW,\%>70}$ Theil-Sen slopes as
470 $\overline{\Delta O_{3,DOW}}$ Theil-Sen slopes, as evidenced by the increased scatter in the right-hand panel of Figure 11 compared to the

471 left-hand panel. Some areas have few exceedances of the NAAQS in the later years of the trends period and this small
 472 sample size could explain the difference between the monitored and modeled slopes, given that the model predicted
 473 fewer exceedance days than were observed in many areas.
 474
 475



476
 477 **Figure 11. Comparison of modeled and observed Theil-Sen slopes in May-Sep WE-WD MDA8 O₃ differences across all**
 478 **nonattainment areas for $\Delta\overline{O_{3,DOW}}$ (left panel) and $\Delta O_{3,DOW,\%>70}$ (right panel). WE-WD differences for the 2002-2005 time-**
 479 **period are indicated by the color bar with positive differences (NO_x-saturated areas) shown in shades of yellow and brown**
 480 **and negative differences (NO_x-limited areas) shown in shades of blue. Note that the brown symbol at the bottom-left of both**
 481 **panels represents the Los Angeles nonattainment area.**
 482

483 Figure 12 shows the comparison of $\Delta\overline{O_{3,DOW}}$ Theil-Sen slopes by season. The summer plot looks similar to the May-
 484 September plot shown in Figure 11. Winter, spring, and fall data show median $\Delta\overline{O_{3,DOW}}$ near zero or greater than zero
 485 in most nonattainment areas suggesting transitional or NO_x-saturated conditions in these seasons. Both observations
 486 and model predictions suggest $\Delta\overline{O_{3,DOW}}$ negative Theil-Sen slopes in these seasons suggesting that nonattainment
 487 areas in the US may be transitioning towards NO_x-limited conditions even outside of the summer ozone season.
 488



489
 490 **Figure 12.** Comparison of modeled and observed $\Delta \overline{O_{3,DOW}}$ Theil-Sen slopes across all nonattainment areas in winter (top
 491 left), spring (top right), summer (bottom left) and fall (bottom right). WE-WD differences for the 2002-2005 time-period
 492 are indicated by the color bar with positive differences (NO_x-saturated areas) shown in shades of yellow and brown and
 493 negative differences (NO_x-limited areas) shown in shades of blue. Note that year-round ozone monitoring is not required
 494 in some parts of the US and therefore monitoring data may not be available outside the May-September period in some
 495 areas.

496 **4 Conclusions**

497
 498 While this assessment has provided insight into the ozone formation regimes across high-ozone locations in the US,
 499 some key questions remain about the important drivers for year-to-year changes in DOW MDA8 ozone patterns and
 500 which of those drivers are well captured by the EQUATES dataset. First, while NO_x and VOC emissions have been
 501 steadily decreasing across most areas of the US, exceptions to that pattern include increasing wildfire emissions

502 especially in the Western US and increasing emissions from oil and gas activities near US nonattainment areas in
503 Texas, Colorado, New Mexico and Utah. Future work could focus on areas impacted by these two emissions sources
504 to assess both the impact of these increasing emissions on ozone formation regimes and the ability of the EQUATES
505 dataset to capture those impacts. Second, this assessment predominantly focused on MDA8 ozone values across the
506 May-Sep ozone season, however, past work has identified some seasonally varying ozone biases within the CMAQ
507 model (Appel et al., 2021). Specifically, EQUATES has a tendency to underpredict ozone during the spring and
508 overpredict ozone later in the summer (Figures S-40 and S-41). Given that ozone formation tends to be more NO_x-
509 saturated in the springtime than in the summer (Jin et al., 2020; Jin et al., 2017), a more in-depth assessment would
510 be needed to fully characterize the extent that differences in observed and modeled WE-WD MDA8 ozone differences
511 are impacted by this seasonally varying model performance. Third, we assessed DOW MDA8 ozone patterns across
512 multiple complex urban areas that encompassed spatially heterogeneous emissions sources and meteorology. For some
513 of these areas (e.g. Los Angeles, CA and Denver, CO) the sign of the Theil-Sen slopes in WE-WD MDA8 ozone
514 appeared consistent across monitoring locations while in others (e.g. New York City, NY) different monitoring
515 locations across the area appeared to show different types of trends. Further local scale investigation into each of these
516 areas would be necessary to fully characterize the nuances of DOW and year-to-year variations in emission and
517 meteorology that obscure the MDA8 ozone DOW trends in some areas but not others when aggregating across monitor
518 locations in those areas. Finally, an intriguing trend in MDA8 ozone DOW patterns was identified in multiple rural
519 and agricultural areas of California. Recent literature has suggested that soil NO emissions, which are unlikely to have
520 a DOW emissions pattern, are an important NO_x emissions source in agricultural locations of California (Almaraz et
521 al., 2018; Zhu et al., 2023). Could the MDA8 ozone DOW trends observed in these areas be reflective of the increasing
522 relative importance of NO_x sources other than mobile sources in those locations? More assessment is needed to
523 definitively determine whether the trend in a decreasing weekday effect is a reliable indicator of areas that are
524 becoming more dominated by local NO_x sources that do not vary by DOW, more dominated by transported ozone, or
525 some other factor. It is important to note that transported ozone may come from nearby regional sources or from longer
526 range sources provided the transport times are sufficient to mask any DOW patterns that would be evident in the
527 source region.

528
529 In this analysis we found that trends in ozone formation chemistry may not always be clearly shown by trends in DOW
530 patterns which are impacted by a complex set of local factors including meteorology, the mix of local emissions
531 sources and monitor locations in relationship to land-water interfaces. Lack of trends appear more often using observed
532 data than modeled data (Figures 4 and 5) meaning that, while the model accurately captures Theil-Sen slopes for
533 $\overline{\Delta O_{3,DOW}}$ and $\Delta O_{3,DOW,\%>70}$ (Figure 11), lower P-values are less common using observational data. This suggests that
534 there may be some stochastic processes making observed year-to-year WE-WD MDA8 ozone differences noisy which
535 are not fully captured by the model. Even with these limitations, this analysis has shown that DOW patterns in ambient
536 NO_x concentrations persist in US urban areas but have become less prominent in some areas while others have
537 transitioned from positive WE-WD MDA8 ozone differences to negative WE-WD MDA8 ozone differences over the
538 18-year period analyzed. These DOW NO_x differences have resulted in distinctive DOW MDA8 ozone patterns in

539 many of the nonattainment areas assessed. The EQUATES modeling simulations appear to show larger and more
540 positive WE-WD MDA8 ozone differences than observational data suggesting that ozone formation in this modeling
541 dataset is less NO_x-limited than in the observations. Despite this discrepancy, the EQUATES dataset captures year-
542 to-year changes in WE-WD MDA8 ozone patterns as demonstrated by high correlation of the Theil-Sen slopes for
543 WE-WD MDA8 ozone differences. The agreement between the modeled and observation datasets are more apparent
544 when assessing summertime mean MDA8 ozone than when analyzing extreme values using the percentage of
545 exceedance days metric. Assessing frequencies or magnitudes of extreme values is challenging using a dataset with a
546 limited number of weekend and weekday days due to the stochastic and infrequent nature of high ozone events in
547 many areas.

548
549 While there are multiple types of measurements and modeling assessments that can be applied to characterize local
550 ozone formation regimes, many of these require specialized measurements or datasets that are not readily available in
551 all areas. In contrast, assessing DOW MDA8 ozone patterns requires only routine daily ozone measurements that are
552 widely available across urban areas in the US and in other countries. Consequently, this type of assessment is a useful
553 tool and may be applied in many areas using routine measurements. In locations with long-term measurements, DOW
554 patterns offer a method to look at trends in ozone formation chemistry over time. While DOW patterns in MDA8
555 ozone are especially useful given the wide availability of data required for this type of assessment, we anticipate that
556 in the near future additional datasets for assessing ozone chemical formation regimes will become more widely
557 available. Specifically, O₃, NO₂ and HCHO data from the recently launched TEMPO satellite may provide the ability
558 to better understand the relationships between WE-WD MDA8 ozone patterns and precursor concentrations.

559 **Author contributions**

560 All authors contributed to conceptualization of the project. HS, CH, KF, BW, and WA contributed to data curation.
561 HS conducted formal analysis. HS, CH, AW, KF, BW, BH, and SK contributed to developing the methodology.
562 HS and BW developed software for performing the analysis. HS, CH, AW, JL, NP, BW, and GT contributed to
563 validation. HS, BW, and BH helped visualize the data. All authors contributed to the writing and editing of the
564 manuscript.

565 **Competing interests**

566 The authors declare that they have no conflict of interest.

567 **Data accessibility statement**

568 The observed and CMAQ estimated gas species data and meteorological data that were used in the analysis are
569 available at <https://doi.org/10.5281/zenodo.10222897>.

570 **Disclaimer:** The views expressed in this manuscript are those of the authors and do not necessarily reflect the views
571 or policies of the U.S. Environmental Protection Agency.

572 **Acknowledgements**

573 The authors would like to acknowledge Chris Nolte and Golam Sarwar for helpful comments on this manuscript. We
574 thank Daniel Jaffe, David Parish, and the anonymous reviewer for their helpful comments through ACP's open
575 discussion review.

576 **References**

- 577 Adame, J. A., Hernández-Ceballos, M. Á., Sorribas, M., Lozano, A., and Morena, B. A. D. I.: Weekend-
578 Weekday Effect Assessment for O₃, NO_x, CO and PM₁₀ in Andalusia, Spain (2003-2008), *Aerosol and Air*
579 *Quality Research*, 14, 1862-1874, 10.4209/aaqr.2014.02.0026, 2014.
- 580 Almaraz, M., Bai, E., Wang, C., Trousdell, J., Conley, S., Faloona, I., and Houlton, B. Z.: Agriculture is a
581 major source of NO_x pollution in California, *Science Advances*, 4, eaao3477,
582 doi:10.1126/sciadv.aao3477, 2018.
- 583 Appel, K. W., Bash, J. O., Fahey, K. M., Foley, K. M., Gilliam, R. C., Hogrefe, C., Hutzell, W. T., Kang, D.,
584 Mathur, R., Murphy, B. N., Napelenok, S. L., Nolte, C. G., Pleim, J. E., Pouliot, G. A., Pye, H. O. T., Ran, L.,
585 Roselle, S. J., Sarwar, G., Schwede, D. B., Sidi, F. I., Spero, T. L., and Wong, D. C.: The Community
586 Multiscale Air Quality (CMAQ) model versions 5.3 and 5.3.1: system updates and evaluation, *Geosci.*
587 *Model Dev.*, 14, 2867-2897, 10.5194/gmd-14-2867-2021, 2021.
- 588 Atkinson-Palombo, C. M., Miller, J. A., and Balling, R. C.: Quantifying the ozone “weekend effect” at
589 various locations in Phoenix, Arizona, *Atmospheric Environment*, 40, 7644-7658,
590 <https://doi.org/10.1016/j.atmosenv.2006.05.023>, 2006.
- 591 Blanchard, C. L. and Tanenbaum, S.: Weekday/Weekend Differences in Ambient Air Pollutant
592 Concentrations in Atlanta and the Southeastern United States, *Journal of the Air & Waste Management*
593 *Association*, 56, 271-284, 10.1080/10473289.2006.10464455, 2006.
- 594 Blanchard, C. L., Tanenbaum, S., and Lawson, D. R.: Differences between Weekday and Weekend Air
595 Pollutant Levels in Atlanta; Baltimore; Chicago; Dallas–Fort Worth; Denver; Houston; New York; Phoenix;
596 Washington, DC; and Surrounding Areas, *Journal of the Air & Waste Management Association*, 58, 1598-
597 1615, 10.3155/1047-3289.58.12.1598, 2008.
- 598 Bruntz, S. M., Cleveland, W. S., Graedel, T. E., Kleiner, B., and Warner, J. L.: OZONE CONCENTRATIONS IN
599 NEW-JERSEY AND NEW-YORK - STATISTICAL ASSOCIATION WITH RELATED VARIABLES, *Science*, 186, 257-
600 259, 10.1126/science.186.4160.257, 1974.
- 601 Chinkin, L. R., Coe, D. L., Funk, T. H., Hafner, H. R., Roberts, P. T., Ryan, P. A., and Lawson, D. R.: Weekday
602 versus Weekend Activity Patterns for Ozone Precursor Emissions in California’s South Coast Air Basin,
603 *Journal of the Air & Waste Management Association*, 53, 829-843, 10.1080/10473289.2003.10466223,
604 2003.
- 605 Cleveland, W. S., Graedel, T. E., Kleiner, B., and Warner, J. L.: SUNDAY AND WORKDAY VARIATIONS IN
606 PHOTOCHEMICAL AIR-POLLUTANTS IN NEW-JERSEY AND NEW-YORK, *Science*, 186, 1037-1038,
607 10.1126/science.186.4168.1037, 1974.
- 608 de Foy, B., Brune, W. H., and Schauer, J. J.: Changes in ozone photochemical regime in Fresno, California
609 from 1994 to 2018 deduced from changes in the weekend effect, *Environmental Pollution*, 263, 114380,
610 <https://doi.org/10.1016/j.envpol.2020.114380>, 2020.
- 611 EPA, U.: EQUATESv1.0: Emissions, WRF/MCIP, CMAQv5.3.2 Data -- 2002-2019 US_12km and
612 NHEMI_108km (V5), UNC Dataverse [dataset], doi:10.15139/S3/F2KJSK, 2021.
- 613 Fisher, R. A.: The Logic of Inductive Inference, *Journal of the Royal Statistical Society*, 98, 39-82,
614 10.2307/2342435, 1935.
- 615 Foley, K. M., Pouliot, G. A., Eyth, A., Aldridge, M. F., Allen, C., Appel, K. W., Bash, J. O., Beardsley, M.,
616 Beidler, J., Choi, D., Farkas, C., Gilliam, R. C., Godfrey, J., Henderson, B. H., Hogrefe, C., Koplitz, S. N.,
617 Mason, R., Mathur, R., Misenis, C., Possiel, N., Pye, H. O. T., Reynolds, L., Roark, M., Roberts, S.,
618 Schwede, D. B., Seltzer, K. M., Sonntag, D., Talgo, K., Toro, C., Vukovich, J., Xing, J., and Adams, E.: 2002–
619 2017 anthropogenic emissions data for air quality modeling over the United States, *Data in Brief*, 47,
620 109022, <https://doi.org/10.1016/j.dib.2023.109022>, 2023.
- 621 Fujita, E. M., Stockwell, W. R., Campbell, D. E., Keislar, R. E., and Lawson, D. R.: Evolution of the
622 Magnitude and Spatial Extent of the Weekend Ozone Effect in California’s South Coast Air Basin, 1981–

623 2000, *Journal of the Air & Waste Management Association*, 53, 802-815,
 624 10.1080/10473289.2003.10466225, 2003a.
 625 Fujita, E. M., Campbell, D. E., Zielinska, B., Sagebiel, J. C., Bowen, J. L., Goliff, W. S., Stockwell, W. R., and
 626 Lawson, D. R.: Diurnal and Weekday Variations in the Source Contributions of Ozone Precursors in
 627 California's South Coast Air Basin, *Journal of the Air & Waste Management Association*, 53, 844-863,
 628 10.1080/10473289.2003.10466226, 2003b.
 629 Gao, H. O.: Day of week effects on diurnal ozone/NO_x cycles and transportation emissions in Southern
 630 California, *Transportation Research Part D: Transport and Environment*, 12, 292-305,
 631 <https://doi.org/10.1016/j.trd.2007.03.004>, 2007.
 632 Gao, H. O. and Niemeier, D. A.: The impact of rush hour traffic and mix on the ozone weekend effect in
 633 southern California, *Transportation Research Part D: Transport and Environment*, 12, 83-98,
 634 <https://doi.org/10.1016/j.trd.2006.12.001>, 2007.
 635 Jaffe, D. A., Ninneman, M., and Chan, H. C.: NO_x and O₃ Trends at U.S. Non-Attainment Areas for 1995–
 636 2020: Influence of COVID-19 Reductions and Wildland Fires on Policy-Relevant Concentrations, 127,
 637 e2021JD036385, <https://doi.org/10.1029/2021JD036385>, 2022.
 638 Jiménez, P., Parra, R., Gassó, S., and Baldasano, J. M.: Modeling the ozone weekend effect in very
 639 complex terrains: a case study in the Northeastern Iberian Peninsula, *Atmospheric Environment*, 39,
 640 429-444, <https://doi.org/10.1016/j.atmosenv.2004.09.065>, 2005.
 641 Jin, X., Fiore, A., Boersma, K. F., Smedt, I. D., and Valin, L.: Inferring Changes in Summertime Surface
 642 Ozone–NO_x–VOC Chemistry over U.S. Urban Areas from Two Decades of Satellite and Ground-Based
 643 Observations, *Environmental Science & Technology*, 54, 6518-6529, 10.1021/acs.est.9b07785, 2020.
 644 Jin, X., Fiore, A. M., Murray, L. T., Valin, L. C., Lamsal, L. N., Duncan, B., Folkert Boersma, K., De Smedt, I.,
 645 Abad, G. G., Chance, K., and Tonnesen, G. S.: Evaluating a Space-Based Indicator of Surface Ozone-NO_x-
 646 VOC Sensitivity Over Midlatitude Source Regions and Application to Decadal Trends, *Journal of*
 647 *Geophysical Research: Atmospheres*, 122, 10,439-410,461, <https://doi.org/10.1002/2017JD026720>,
 648 2017.
 649 Kendall, M. G.: *Rank Correlation Methods*, 4th edition, Charles Griffin, London1975.
 650 Koo, B., Jung, J., Pollack, A. K., Lindhjem, C., Jimenez, M., and Yarwood, G.: Impact of meteorology and
 651 anthropogenic emissions on the local and regional ozone weekend effect in Midwestern US,
 652 *Atmospheric Environment*, 57, 13-21, <https://doi.org/10.1016/j.atmosenv.2012.04.043>, 2012.
 653 Koplitz, S., Simon, H., Henderson, B., Liljegren, J., Tonnesen, G., Whitehill, A., and Wells, B.: Changes in
 654 Ozone Chemical Sensitivity in the United States from 2007 to 2016, *ACS Environmental Au*, 2, 206-222,
 655 10.1021/acsenvironau.1c00029, 2022.
 656 Krotkov, N. A., McLinden, C. A., Li, C., Lamsal, L. N., Celarier, E. A., Marchenko, S. V., Swartz, W. H.,
 657 Bucsela, E. J., Joiner, J., Duncan, B. N., Boersma, K. F., Veeffkind, J. P., Levelt, P. F., Fioletov, V. E.,
 658 Dickerson, R. R., He, H., Lu, Z. F., and Streets, D. G.: Aura OMI observations of regional SO₂ and NO₂
 659 pollution changes from 2005 to 2015, *Atmospheric Chemistry and Physics*, 16, 4605-4629, 10.5194/acp-
 660 16-4605-2016, 2016.
 661 Lamsal, L. N., Duncan, B. N., Yoshida, Y., Krotkov, N. A., Pickering, K. E., Streets, D. G., and Lu, Z. F.: U.S.
 662 NO₂ trends (2005-2013): EPA Air Quality System (AQS) data versus improved observations from the
 663 Ozone Monitoring Instrument (OMI), *Atmospheric Environment*, 110, 130-143,
 664 10.1016/j.atmosenv.2015.03.055, 2015.
 665 Mann, H. B.: Nonparametric Tests Against Trend, *Econometrica*, 13, 245-259, 10.2307/1907187, 1945.
 666 Marr, L. C. and Harley, R. A.: Spectral analysis of weekday-weekend differences in ambient ozone,
 667 nitrogen oxide, and non-methane hydrocarbon time series in California, *Atmospheric Environment*, 36,
 668 2327-2335, 10.1016/s1352-2310(02)00188-7, 2002a.

669 Marr, L. C. and Harley, R. A.: Modeling the effect of weekday-weekend differences in motor vehicle
670 emissions on photochemical air pollution in central California, *Environmental Science & Technology*, 36,
671 4099-4106, 10.1021/es020629x, 2002b.

672 Martins, E. M., Nunes, A. C. L., and Correa, S. M.: Understanding Ozone Concentrations During
673 Weekdays and Weekends in the Urban Area of the City of Rio de Janeiro, *Journal of the Brazilian
674 Chemical Society*, 26, 1967-1975, 10.5935/0103-5053.20150175, 2015.

675 Mehta, C. R. and Patel, N. R.: A Network Algorithm for Performing Fisher's Exact Test in $r \times c$ Contingency
676 Tables, *Journal of the American Statistical Association*, 78, 427-434, 10.2307/2288652, 1983.

677 Murphy, J. G., Day, D. A., Cleary, P. A., Wooldridge, P. J., Millet, D. B., Goldstein, A. H., and Cohen, R. C.:
678 The weekend effect within and downwind of Sacramento – Part 1: Observations of ozone,
679 nitrogen oxides, and VOC reactivity, *Atmos. Chem. Phys.*, 7, 5327-5339, 10.5194/acp-7-5327-2007, 2007.

680 Paschalidou, A. K. and Kassomenos, P. A.: Comparison of Air Pollutant Concentrations between
681 Weekdays and Weekends in Athens, Greece for Various Meteorological Conditions, *Environmental
682 Technology*, 25, 1241-1255, 10.1080/09593332508618372, 2004.

683 Pierce, T., Hogrefe, C., Trivikrama Rao, S., Porter, P. S., and Ku, J.-Y.: Dynamic evaluation of a regional air
684 quality model: Assessing the emissions-induced weekly ozone cycle, *Atmospheric Environment*, 44,
685 3583-3596, <https://doi.org/10.1016/j.atmosenv.2010.05.046>, 2010.

686 Pires, J. C. M.: Ozone Weekend Effect Analysis in Three European Urban Areas, *CLEAN – Soil, Air, Water*,
687 40, 790-797, <https://doi.org/10.1002/clen.201100410>, 2012.

688 Plocoste, T., Dorville, J.-F., Monjoly, S., Jacoby-Koaly, S., and André, M.: Assessment of nitrogen oxides
689 and ground-level ozone behavior in a dense air quality station network: Case study in the Lesser Antilles
690 Arc, *Journal of the Air & Waste Management Association*, 68, 1278-1300,
691 10.1080/10962247.2018.1471428, 2018.

692 Pun, B. K., Seigneur, C., and White, W.: Day-of-Week Behavior of Atmospheric Ozone in Three U.S. Cities,
693 *Journal of the Air & Waste Management Association*, 53, 789-801, 10.1080/10473289.2003.10466231,
694 2003.

695 Roberts, S. J., Salawitch, R. J., Wolfe, G. M., Marvin, M. R., Canty, T. P., Allen, D. J., Hall-Quinlan, D. L.,
696 Krask, D. J., and Dickerson, R. R.: Multidecadal trends in ozone chemistry in the Baltimore-Washington
697 Region, *Atmospheric Environment*, 285, 119239, <https://doi.org/10.1016/j.atmosenv.2022.119239>,
698 2022.

699 Rubio, M. A., Sanchez, K., and Lissi, Y. E.: OZONE LEVELS ASSOCIATED TO THE PHOTOCHEMICAL SMOG IN
700 SANTIAGO OF CHILE. THE ELUSIVE ROL OF HYDROCARBONS, *Journal of the Chilean Chemical Society*, 56,
701 709-711, 2011.

702 Russell, A. R., Valin, L. C., and Cohen, R. C.: Trends in OMI NO₂ observations over the United States:
703 effects of emission control technology and the economic recession, *Atmospheric Chemistry and Physics*,
704 12, 12197-12209, 10.5194/acp-12-12197-2012, 2012.

705 Seinfeld, J. H. and Pandis, S. N.: *Atmospheric chemistry and physics: from air pollution to climate change*,
706 John Wiley & Sons 2016.

707 Sen, P. K.: Estimates of the Regression Coefficient Based on Kendall's Tau, *Journal of the American
708 Statistical Association*, 63, 1379-1389, 10.1080/01621459.1968.10480934, 1968.

709 Sillman, S.: THE USE OF NO_Y, H₂O₂, AND HNO₃ AS INDICATORS FOR OZONE-NO_X-HYDROCARBON
710 SENSITIVITY IN URBAN LOCATIONS, *Journal of Geophysical Research-Atmospheres*, 100, 14175-14188,
711 10.1029/94jd02953, 1995.

712 Sillman, S.: The relation between ozone, NO_x and hydrocarbons in urban and polluted rural
713 environments, *Atmospheric Environment*, 33, 1821-1845, 10.1016/s1352-2310(98)00345-8, 1999.

714 Sillman, S., Logan, J. A., and Wofsy, S. C.: THE SENSITIVITY OF OZONE TO NITROGEN-OXIDES AND
715 HYDROCARBONS IN REGIONAL OZONE EPISODES, *Journal of Geophysical Research-Atmospheres*, 95,
716 1837-1851, 10.1029/JD095iD02p01837, 1990.

717 Simon, H., Reff, A., Wells, B., Xing, J., and Frank, N.: Ozone Trends Across the United States over a Period
718 of Decreasing NO_x and VOC Emissions, *Environmental Science & Technology*, 49, 186-195,
719 10.1021/es504514z, 2015.

720 Singh, S. and Kavouras, I. G.: Trends of Ground-Level Ozone in New York City Area during
721 2007–2017, 13, 114, 2022.

722 Theil, H.: A Rank-Invariant Method of Linear and Polynomial Regression Analysis, in: Henri Theil's
723 Contributions to Economics and Econometrics: Econometric Theory and Methodology, edited by: Raj, B.,
724 and Koerts, J., Springer Netherlands, Dordrecht, 345-381, 10.1007/978-94-011-2546-8_20, 1992.

725 Toro, C., Foley, K., Simon, H., Henderson, B., Baker, K. R., Eyth, A., Timin, B., Appel, W., Luecken, D.,
726 Beardsley, M., Sonntag, D., Possiel, N., and Roberts, S.: Evaluation of 15 years of modeled atmospheric
727 oxidized nitrogen compounds across the contiguous United States, *Elementa-Science of the*
728 *Anthropocene*, 9, 10.1525/elementa.2020.00158, 2021.

729 U.S. Environmental Protection Agency: Integrated Science Assessment (ISA) for Particulate Matter (Final
730 report, Dec 2019). U.S. Environmental Protection Agency, Washington, DC, EPA/600/R-19/188, 2019.

731 Warneke, C., de Gouw, J. A., Edwards, P. M., Holloway, J. S., Gilman, J. B., Kuster, W. C., Graus, M., Atlas,
732 E., Blake, D., Gentner, D. R., Goldstein, A. H., Harley, R. A., Alvarez, S., Rappenglueck, B., Trainer, M., and
733 Parrish, D. D.: Photochemical aging of volatile organic compounds in the Los Angeles basin: Weekday-
734 weekend effect, 118, 5018-5028, <https://doi.org/10.1002/jgrd.50423>, 2013.

735 Welch, B. L.: THE GENERALIZATION OF 'STUDENT'S' PROBLEM WHEN SEVERAL DIFFERENT POPULATION
736 VARIANCES ARE INVOLVED, *Biometrika*, 34, 28-35, 10.1093/biomet/34.1-2.28, 1947.

737 Wells, B., Dolwick, P., Eder, B., Evangelista, M., Foley, K., Mannshardt, E., Misenis, C., and Weishampel,
738 A.: Improved estimation of trends in U.S. ozone concentrations adjusted for interannual variability in
739 meteorological conditions, *Atmospheric Environment*, 248, 118234,
740 <https://doi.org/10.1016/j.atmosenv.2021.118234>, 2021.

741 Zhang, G., Sun, Y., Xu, W., Wu, L., Duan, Y., Liang, L., and Li, Y.: Identifying the O₃ chemical regime
742 inferred from the weekly pattern of atmospheric O₃, CO, NO_x, and PM₁₀: Five-year observations at a
743 center urban site in Shanghai, China, *Science of The Total Environment*, 888, 164079,
744 <https://doi.org/10.1016/j.scitotenv.2023.164079>, 2023.

745 Zhu, Q., Place, B., Pfannerstill, E. Y., Tong, S., Zhang, H., Wang, J., Nussbaumer, C. M., Wooldridge, P.,
746 Schulze, B. C., Arata, C., Bucholtz, A., Seinfeld, J. H., Goldstein, A. H., and Cohen, R. C.: Direct
747 observations of NO_x emissions over the San Joaquin Valley using airborne flux measurements during
748 RECAP-CA 2021 field campaign, *Atmos. Chem. Phys. Discuss.*, 2023, 1-21, 10.5194/acp-2023-3, 2023.

749

750

751

752

753

754

755

756

757

758

759

760

761

762

763